

## Solar Chemical Abundances Determined with a CO5BOLD 3D Model Atmosphere

E. Caffau · H.-G. Ludwig · M. Steffen · B. Freytag · P. Bonifacio

Received: 30 October 2009 / Accepted: 5 February 2010 / Published online: 27 March 2010  
© Springer Science+Business Media B.V. 2010

**Abstract** In the last decade, the photospheric solar metallicity as determined from spectroscopy experienced a remarkable downward revision. Part of this effect can be attributed to an improvement of atomic data and the inclusion of NLTE computations, but also the use of hydrodynamical model atmospheres seemed to play a role. This “decrease” with time of the metallicity of the solar photosphere increased the disagreement with the results from helioseismology. With a CO<sup>5</sup>BOLD 3D model of the solar atmosphere, the CIFIST team at the Paris Observatory re-determined the photospheric solar abundances of several elements, among them C, N, and O. The spectroscopic abundances are obtained by fitting the equivalent width and/or the profile of observed spectral lines with synthetic spectra computed from the 3D model atmosphere. We conclude that the effects of granular fluctuations de-

---

Helioseismology

Guest Editors: G. Houdek, H. Shibahashi, and J. Zhao.

E. Caffau (✉) · H.-G. Ludwig · P. Bonifacio

GEPI, Observatoire de Paris, CNRS, Université Paris Diderot; 92195 Meudon Cedex, France

e-mail: [Elisabetta.Caffau@obspm.fr](mailto:Elisabetta.Caffau@obspm.fr)

url: <http://cifist.obspm.fr>

H.-G. Ludwig · P. Bonifacio

CIFIST Marie Curie Excellence Team, Observatoire de Paris, 92195 Meudon Cedex, France

H.-G. Ludwig

Zentrum für Astronomie der Universität Heidelberg, Landessternwarte, Königstuhl 12,  
69117 Heidelberg, Germany

M. Steffen

Astrophysikalisches Institut Potsdam, An der Sternwarte 16, 14482 Potsdam, Germany

B. Freytag

CRAL, UMR 5574: CNRS, Université de Lyon, École Normale Supérieure de Lyon, 46 allée d'Italie,  
69364 Lyon Cedex 7, France

P. Bonifacio

Istituto Nazionale di Astrofisica, Osservatorio Astronomico di Trieste, Via G.B. Tiepolo 11,  
34143 Trieste, Italy

pend on the characteristics of the individual lines, but are found to be relevant only in a few particular cases. 3D effects are not responsible for the systematic lowering of the solar abundances in recent years. The solar metallicity resulting from this analysis is  $Z = 0.0153$ ,  $Z/X = 0.0209$ .

**Keywords** Sun: abundances · Sun: photosphere · Line: formation · Hydrodynamics · Convection · Radiative transfer

## 1. Introduction

Since the pioneering work of Russell (1929), the study of the chemical composition of the solar photosphere has been an important topic in astronomy. Russell, measuring the strength of the absorption lines in the observed solar spectrum, determined the abundance of 56 elements and six molecules. After this work many other astronomers analysed the solar spectrum in order to deduce the detailed pattern of photospheric abundances. The accurate determination of the solar chemical abundances is a major topic, because:

- i) the knowledge of the elemental abundances in the present solar photosphere is the basis to infer the chemical composition of the initial Sun, and allows one to reconstruct the past and future evolution of the Sun, including its physical and chemical internal structure;
- ii) the comparison of the chemical abundances in the solar photosphere and in meteoritic samples provides important information about the formation and chemical evolution of the solar system;
- iii) the construction of detailed models of the solar atmosphere requires the knowledge of its chemical composition;
- iv) the knowledge of the solar photospheric chemical abundance allows for the empirical determination of the oscillator strength of any spectral line of this element observable in the solar spectrum;
- v) the solar abundances serve as a reference for the chemical analysis of other stars in the Galaxy, of the interstellar medium, and of the stellar populations of external galaxies.

In our analysis of the solar photosphere we are mainly interested in the first and third points.

For our work on the solar abundance determinations, we rely on a CO<sup>5</sup>BOLD 3D model of the solar photosphere. We were interested to understand if the presence of horizontal fluctuations (the solar granulation) has a systematic effect on the abundances derived from the 3D model with respect to what is obtained by 1D models which ignore granulation.

We find that the effects of granular fluctuations can lead to both positive and negative abundance corrections, depending on the properties of the individual spectral line under consideration. However, the granulation effect is relevant only in a few particular cases. 3D effects are not responsible for the systematic lowering of the solar abundances in recent years.

In the following sections we summarise the investigations of some elements that we have already published and present a new analysis of some other elements (Li, K, Fe, and Os). For a complete overview of the solar abundance determinations we recommend the review by Lodders, Palme, and Gail (2009) as a very detailed and complete work.

## 2. Model Atmospheres

Our abundance analyses of the solar photosphere are based on a time-dependent, 3D, hydrodynamical model atmosphere computed with the CO<sup>5</sup>BOLD code [<http://www.astro.uu.se/>]

[~bf/co5bold\\_20020216/cobold.html](#)] (Freytag, Steffen, and Dorch, 2002; Freytag *et al.*, 2003). The 3D model atmosphere we use has a box size of  $5.6 \times 5.6 \times 2.27 \text{ Mm}^3$ , a resolution of  $140 \times 140 \times 150$  grid points, and spans a range in optical depth of about  $-6.7 < \log \tau_{\text{Ross}} < 5.5$  (from  $-1.4 \text{ Mm}$  below to  $+0.9 \text{ Mm}$  above  $\tau_{\text{Ross}} = 1$ ). The selected 19 snapshots we use for the spectrum-synthesis calculations are equidistantly spaced in time, sufficiently separated in time to show little correlation, and cover 1.2 hours of solar time. For comparison, the following 1D plane-parallel model atmospheres were considered:

- i) the (3D) model obtained by horizontally averaging each 3D snapshot over surfaces of equal (Rosseland) optical depth;
- ii) the 1D<sub>LHD</sub> model, a 1D hydrostatic mixing-length model which employs the same micro-physics and radiative transfer scheme as CO<sup>5</sup>BOLD;
- iii) the semi-empirical Holweger–Müller solar model (Holweger, 1967; Holweger and Müller, 1974, hereafter HM);
- iv) the ATLAS-9 model computed by F. Castelli [<http://www.user.oats.inaf.it/castelli/sun/ap00t5777g44377k1asp.dat>] with the solar abundances of Asplund, Grevesse, and Sauval (2005).

The (3D) and 1D<sub>LHD</sub> models have been introduced as reference 1D models, because they share the microphysics with the 3D model (Caffau and Ludwig, 2007). For more details about the 1D and 3D models used in our analysis see Caffau *et al.* (2008a) or the other papers of the collaboration on the determination of the solar photospheric abundances.

### 3. 3D Corrections

We investigated the effects of 3D convection on solar abundances in Caffau, Ludwig, and Steffen (2009). To define 3D corrections we selected two reference models: (3D) and 1D<sub>LHD</sub>. Both share the microphysics of the 3D-CO<sup>5</sup>BOLD model to ensure differential comparability. We distinguish two different 3D corrections, defined as:  $\Delta^{(1)}(\xi_{\text{mic}}) = A(Y)_{3D} - A(Y)_{(3D)}$  and  $\Delta^{(2)}(\xi_{\text{mic}}, \alpha_{\text{MLT}}) = A(Y)_{3D} - A(Y)_{1D_{\text{LHD}}}$ , where  $Y$  represents any chemical element, and  $A(Y) = \log(n_Y/n_H) + 12$ . The first correction isolates the granulation effects, *i.e.* the influence of the horizontal fluctuations around the mean stratification, while the second one measures the total 3D effect, accounting for both horizontal fluctuations and for the different influence of 3D hydrodynamical and 1D mixing-length convection, respectively, on the resulting *mean* temperature structure. Obviously, both 3D corrections depend on the choice of the microturbulence parameter  $[\xi_{\text{mic}}]$  used with the 1D models, while the second one is also a function of the mixing-length parameter  $[\alpha_{\text{MLT}}]$  adopted for the 1D<sub>LHD</sub> model. The idea is that these 3D corrections can be derived from the simulations with much better accuracy than the detailed thermal structure of the solar atmosphere in absolute terms. While the latter depends sensitively on, *e.g.*, the frequency binning adopted for the radiation hydrodynamics, the 3D corrections are less sensitive to such details, as they are defined in a strictly differential way. Hence, the 3D corrections are not merely evaluated to measure the abundance difference between a given pair of 3D and 1D models, but they may rather be utilised to improve the abundance determinations from standard 1D models. Abundances derived from the semi-empirical HM model should be corrected by adding only the “granulation correction”  $\Delta^{(1)}(\xi_{\text{mic}})$ , while abundances based on standard 1D mixing-length models such as ATLAS or MARCS must be corrected by adding the “total 3D correction”  $\Delta^{(2)}(\xi_{\text{mic}}, \alpha_{\text{MLT}})$ .

The 3D corrections are well defined as long as the lines considered are weak such that their equivalent widths are independent of the assumed microturbulence. The situation becomes more problematic once the lines are partly saturated, because then the corrections

depend on  $\xi_{\text{mic}}$ , and the choice of the microturbulence parameter is critical. In principle, the microturbulence parameter derived empirically from analysing observed solar spectra with a standard 1D model [ $\xi_{\text{mic}}(\text{Sun-1X})$ ] should be identical to the theoretical microturbulence [ $\xi_{\text{mic}}(\text{Hydro-1D}_{\text{LHD}})$ ] obtained from analysing the synthetic spectrum of the 3D hydrodynamical model atmosphere with the 1D<sub>LHD</sub> model. However, there are indications that  $\xi_{\text{mic}}(\text{Hydro-1D}_{\text{LHD}})$  is systematically smaller than  $\xi_{\text{mic}}(\text{Sun-1X})$  (Steffen, Ludwig, and Caffau, 2009). As a consequence, the 3D corrections should be computed with  $\xi_{\text{mic}}(\text{Hydro-1D}_{\text{LHD}})$ . Wherever possible, abundances from weak lines are to be preferred.

For some of the weak lines that we investigated (*e.g.* the C I line at 538 nm), we compared the 3D correction  $\Delta^{(1)}$  with the results of Steffen and Holweger (2002), which are based on a 2D hydrodynamical simulation and find a close agreement. Summarising our analysis, we can say that the total 3D correction  $\Delta^{(2)}$  is positive for the majority of the relevant spectral lines, except for a few weak, high-excitation lines (mostly nitrogen) for which both  $\Delta^{(1)}$  and  $\Delta^{(2)}$  are negative. However, the 3D corrections are small in general.

The abundances presented in this work have been derived directly from the 3D model, in line with our previous publications. We trust in the temperature structure of our 3D-CO<sup>5</sup>BOLD model, because it is able to reproduce the centre-to-limb variation of the continuum intensity even somewhat better than the HM model (Ludwig *et al.*, 2010). However, we plan to compute abundances also with the alternative approach, *i.e.* from the HM model and correcting by  $\Delta^{(1)}(\xi_{\text{mic}})$ , in future investigations. While it is not entirely clear which of the two approaches gives the more reliable results, we propose the abundance differences between the two methods to be considered as a measure of the systematic uncertainty of the abundance analysis.

#### 4. Observational Data

Our analysis is based mainly on four high resolution, high signal-to-noise ratio [S/N] spectra, two for disc centre, and two for the integrated disc. For most elements that we use more than one solar spectrum, because we realised that the abundances derived from different spectra do not always agree within one  $\sigma$ . The observed spectra we considered are:

- i) the integrated-disc spectrum based on fifty solar FTS scans taken by J. Brault and L. Testerman at Kitt Peak between 1981 and 1984 (Kurucz, 2005);
- ii) the two absolutely calibrated FTS spectra obtained at Kitt Peak in the 1980s, covering the range 330 nm to 1250 nm for the integrated disc and disc centre (Neckel and Labs, 1984; Neckel, 1999);
- iii) the disc-centre intensity spectrum in the range 300 nm to 1000 nm observed from the Jungfrauoch (Delbouille, Roland, and Neven, 1973), and in the range from 1000 nm to 5400 nm observed from Kitt Peak (Delbouille *et al.*, 1981).

#### 5. Chemical Abundances

##### 5.1. Lithium

Lithium is widely studied in metal-poor stars. The Li I resonance doublet at 670.7 nm is also observable in the solar spectrum and in the spectra of F–K main-sequence stars. In metal-poor stars, this region is very clean, and the lithium feature is not blended. This is not the case in solar-metallicity stars, where atomic and molecular lines contaminate the

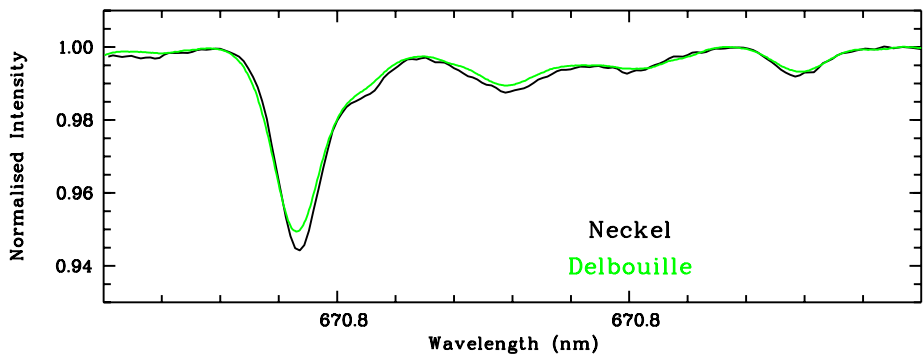


**Figure 1** Comparison of the two atlases of the solar disc centre in the region of the Li I line.

region. Good atomic data for these blending lines are not readily available in databases, but there are a few published line lists that have been used for the abundance analysis of the solar photosphere. For our own analysis of Li in the solar photosphere, we took into account both granulation and 3D-NLTE (Non Local Thermodynamic Equilibrium) effects in computing the contribution of the Li doublet, while 3D-LTE line-formation calculations were performed for the other blend components.

Considering the four solar atlases described above to investigate lithium, we realise that the two observed intensity spectra are significantly different (see Figure 1). We have no explanation for this disagreement. The easiest way to explain it would be to invoke telluric absorption, but this spectral range has been carefully scrutinised in the context of the Li isotopic ratio in metal-poor stars, and it seems unlikely that a telluric absorption could have gone unnoticed. We decided to discard the Delbouille disc-centre atlas, and to work only with the other three atlases for the Li abundance determination. The reason for discarding the Delbouille disc-centre atlas is that we cannot reproduce the profile with synthetic spectra, while we can in the case of the other three solar atlases, and obtain Li abundances that agree closely.

The two lists of blending lines that can reproduce the solar spectrum in this region reasonably well are those from Ghezzi *et al.* (2009) and from Reddy *et al.* (2002). To obtain the Li abundance, we fit the observed line profile, interpolating in a grid of 3D synthetic spectra, in which NLTE effects are taken into account for Li. We obtain  $A(\text{Li})_{3\text{D-NLTE}} = 1.03 \pm 0.03$ , fitting the three observed line profiles using the Ghezzi *et al.* (2009) line list. Fortunately, the solar lithium abundance is not very sensitive to the choice between the two line lists: when using the list due to Reddy *et al.* (2002), we obtain  $A(\text{Li})_{3\text{D-NLTE}} = 1.01$ .

## 5.2. Carbon

For a selection of 45 lines, we measured the equivalent widths, taking into account the blending components, when present, and we obtained  $A(\text{C}) = 8.50 \pm 0.06$  (Caffau *et al.*, 2010). NLTE corrections were computed with the Kiel code (Steenbock and Holweger, 1984), using the (3D) model as input. In our sample of C I lines there is one forbidden line at 872.7 nm, formed in LTE conditions. Its abundance of  $A(\text{C}) = 8.48 \pm 0.02$  is very close to the value we obtain from the complete sample. A considerable fraction of our selected lines are strong, in the saturated part of the curve of growth. We do not see a trend of the carbon abundance with respect to the equivalent widths of the lines, and the  $A(\text{C})$  is unchanged if we consider

only lines whose EW is smaller than 12 pm. When we consider lines weaker than 8 pm equivalent width,  $A(C)$  is lower by 0.02 dex.

### 5.3. Nitrogen

Our analysis relies on two sets of equivalent-width measurements (Biémont *et al.*, 1990; Grevesse *et al.*, 1990). The nitrogen abundance is obtained by interpolating in synthetic curves-of-growth from 3D and 1D models. To account for NLTE effects, we applied the corrections computed in using the  $\langle 3D \rangle$  as the 1D background stratification. The result is  $A(N) = 7.86 \pm 0.12$ , as reported in detail by Caffau *et al.* (2009) and Maiorca *et al.* (2009). Asplund *et al.* (2009) criticise our line selection, but unfortunately provide no information on their own analysis, except their line-to-line scatter of 0.04 dex. We note that the difference between the abundance from their atomic and molecular NH  $\Delta v = 1$  lines is about 0.1 dex.

### 5.4. Oxygen

Our photospheric oxygen abundance of  $8.76 \pm 0.07$  is derived from ten atomic oxygen lines. The NLTE corrections are computed from the  $\langle 3D \rangle$  model as input to the Kiel code, and applied to the 3D-LTE abundances. For details of the analysis see Caffau *et al.* (2008a) and Caffau and Ludwig (2008). In our analysis we find a disagreement between the two forbidden [O I] lines at 630 nm and 636 nm of more than 0.1 dex that we are not able to explain, unless we allow the contribution of the nickel blend of the line at 630 nm to be smaller than expected by about a factor of two (see also Ayres, 2008). Interestingly, Lambert (1978) already considered the presence of the Ni I line, but concluded that such a contribution must be small to have an agreement between the two [O I] lines. This disagreement is not present in Asplund *et al.* (2004), while in Asplund *et al.* (2009) a disagreement is recognised, but no solution is offered. When we use the equivalent widths given by Asplund *et al.* (2004) together with our 3D model, we indeed find an agreement between the two lines, but with a “high”  $A(O)$  value of 8.79 and 8.76, respectively, while Asplund *et al.* (2004) give  $A(O) = 8.69$  and 8.67 for the two forbidden lines. This difference is probably related to differences in the temperature structure of the two independent 3D model atmospheres.

### 5.5. Phosphorus

We considered five infrared P I lines of Multiplet 1 for the photospheric abundance determination (Caffau *et al.*, 2007b). Our photospheric phosphorus abundance of  $A(P) = 5.46 \pm 0.04$  is in perfect agreement with the meteoritic value (Lodders, Palme, and Gail, 2009). The phosphorus abundance in Asplund *et al.* (2009) is 0.06 dex larger with respect to the value of  $A(P) = 5.35 \pm 0.04$  given in Asplund, Grevesse, and Sauval (2005). It is unclear whether this upward revision is related to their new 3D model or to a change in the line list, in the  $\log gf$  values, and/or the adopted equivalent widths.

### 5.6. Sulphur

In Lodders, Palme, and Gail (2009) the photospheric sulphur abundance is given as  $A(S) = 7.14 \pm 0.01$  and the meteoritic one as  $A(S) = 7.17 \pm 0.02$ . We have studied several S I lines in the solar spectrum. From the weak forbidden line at 1082 nm we obtain  $A(S) = 7.15 \pm (0.01)_{\text{stat}} \pm (0.05)_{\text{sys}}$  (Caffau and Ludwig, 2007). Asplund *et al.* (2009) criticise both the measured equivalent widths as being too small, and the  $\log gf$  we (and also

Ryde, 2006) use as being obsolete, claiming that updated values should be used. As no further details are given, it is impossible to judge whether their equivalent widths and  $\log gf$  values are better. We considered also the permitted lines of Multiplet 3, Multiplet 6, and Multiplet 8, discarding the strong lines of Multiplet 1 at 920 nm, because they are blended with telluric absorption (Caffau *et al.*, 2007a). Both lines of Multiplet 6 and Multiplet 8 are weak and close to LTE. The abundance we find is  $A(S) = 7.14$  from the line of Multiplet 8, and  $A(S) = 7.11$  from the two lines of Multiplet 6. The lines of Multiplet 3 at 1045 nm are affected by departures from LTE. If we take this effect into account, using the NLTE correction of Takeda *et al.* (2005), we obtain  $A(S) = 7.30$ . This value becomes  $A(S) = 7.28$  when using the NLTE corrections computed by Andrievsky and Korotin with the sulphur model atom described in Korotin (2008) and Korotin (2009). The simple average over all of the multiplets would give  $A(S) = 7.17 \pm 0.07$ , where  $\sigma$  is the root-mean-square deviation. Giving twice the weight to the [Si] lines and the lines of Multiplet 8 because they are unaffected by NLTE, we obtain  $A(S) = 7.16 \pm 0.05$ , which we recommend as the solar photospheric value.

### 5.7. Potassium

In the solar spectrum, potassium is observed through lines of the neutral species, K I. As for other alkalis, the strongest lines are those of the resonance doublet of K I at 766.4 nm and 769.8 nm, the only observable lines in metal-poor stars. In fact, the other K I lines are much weaker. Unfortunately, the strongest K I line at 766.4 nm is heavily blended in the solar spectrum by strong telluric O<sub>2</sub> absorption.

De La Reza and Müller (1975) performed the first detailed study of the K I 769.8 nm doublet component in the solar photosphere, analysing its centre-to-limb variation and computing the K abundance in NLTE.

Among the few excited K I lines, the one at 404.4 nm is often used in old solar abundance analyses; but this line is significantly blended and the  $f$  value is uncertain so that it is excluded by de La Reza and Müller (1975). Also Lambert and Luck (1978) suggest that an incorrect  $f$  value could be the reason for the exceedingly low abundance derived from this line.

Takeda *et al.* (1996) obtain a good fit of the solar flux spectrum with their synthetic profile of the line at 769.8 nm with a multi-parameter fitting method. They also studied the dependence of the K abundance upon the atomic parameters, the microturbulence, and the adopted model atmosphere (see their Table 4). The NLTE correction for this line is estimated by them to be about  $-0.4$  dex.

Zhang *et al.* (2006) consider seven lines: the line at 693.8 nm, the resonance doublet, plus four lines in common with Lambert and Luck (1978). These authors derive the potassium abundance by line profile fitting of the integrated-disc solar spectrum with a NLTE synthetic profile. The NLTE corrections provided in this paper are applied to our LTE analysis (see below). Takeda *et al.* (1996) select eight weak K lines, adding to the list of Zhang *et al.* (2006) the lines at 404.7, 533.9, and 583.1 nm, while they ignore the 1243.2 nm line, which is included by Zhang *et al.* (2006). According to Ivanova and Shimanskiĭ (2000) NLTE corrections are small for the 693.8 nm line, important for the 1252.2, 1243.2, and 1176.9 nm lines, and very important for the 769.8 nm line.

Our present analysis is based on the six K I lines listed in Table 1. By means of the IRAF task *splot* [<http://iraf.noao.edu/>], we have measured the equivalent widths in the observed solar atlases. Interpolating in the curve of growth, we determine the potassium abundance in the solar photosphere from both 3D and 1D model atmospheres. NLTE corrections were



**Table 1** Atomic data and derived abundances for our selection of K I lines

$\lambda$ nm	$\chi$ eV	$\log gf$	$A(K)$			
			3D-LTE	(3D)-LTE	1D <sub>LHD</sub> -LTE	3D-NLTE
580.1749	1.617	2.20	5.263	5.279	5.225	5.203
693.8763	1.617	4.00	4.998	5.017	4.962	4.929
769.8974	0.000	170.00	5.434	5.458	5.353	5.144
1176.9689	0.000	50.00	5.329	5.359	5.288	5.199
1243.2273	1.617	56.00	5.279	5.308	5.237	5.129
1252.2134	1.610	85.00	5.275	5.304	5.222	5.055
$\langle A(K) \rangle$			5.263	5.296	5.223	5.110

taken from Zhang *et al.* (2006) where available. The NLTE K abundance derived from the 1D<sub>LHD</sub> model (with  $\xi_{\text{mic}} = 1.0 \text{ km s}^{-1}$ ),  $A(K) = 5.06 \pm 0.04$ , is in good agreement with the value of  $A(K) = 5.12 \pm 0.03$  obtained by Zhang *et al.* (2006) by using the Kitt Peak integrated-disc atlas, and excluding the uncertain 766.4 nm line. The potassium abundance given by Lodders, Palme, and Gail (2009) is  $A(K) = 5.12 \pm 0.03$ , while Asplund *et al.* (2009) recommend  $A(K) = 5.03 \pm 0.09$ .

Our adopted value is  $A(K)_{\text{3D-NLTE}} = 5.11 \pm 0.09$ , which is obtained by applying the NLTE corrections of Zhang *et al.* (2006) to the results from the 3D-LTE analysis for the integrated-disc spectrum. The 3D-LTE results from disc centre and integrated disc agree very closely, the latter being 0.03 dex higher. This tiny difference is probably due to different NLTE corrections.

## 5.8. Iron

Iron is a complex atom with a very rich spectrum of atomic lines, especially from the neutral and singly ionised stage. Many scientists have studied the determination of the iron abundance in the solar photosphere, both from Fe I (which accounts for most of the lines in the solar spectrum) and from Fe II (which is the dominant ionisation stage of iron in the photosphere).

The iron abundance was continuously decreasing from the value given by Russell (1929) until the 1960s. The correction of the transition probabilities produced an increasing solar abundance by about one order of magnitude until the 1990s. Since then,  $A(\text{Fe})$  has experienced a smooth decrease (see Figure 1 in Grevesse and Sauval, 1999). We recall some important developments in this field: Corliss and collaborators investigated the iron abundance, with their transition probability (Corliss and Warner, 1966; Corliss and Tech, 1968); Bridges and coworkers applied their new  $gf$ -scale to the abundance determination (Bridges and Wiese, 1970; Bridges and Kornblith, 1974). Between 1980–1990, there was a long debate between Holweger and the Blackwell group, advocating a low ( $A(\text{Fe}) = 7.50$ ) and a high ( $A(\text{Fe}) = 7.63$ ) iron abundance, respectively (Biemont *et al.*, 1991; Blackwell, Lynas-Gray, and Smith, 1995; Holweger, Kock, and Bard, 1995; Blackwell, Smith, and Lynas-Gray, 1995; Kostik, Shchukina, and Rutten, 1996). Kostik, Shchukina, and Rutten (1996) pointed out the necessity of performing a 3D-NLTE analysis, which was impossible at the time for lack of computer power and atomic-physics data.

To investigate the iron abundance in the solar photosphere, we selected 15 Fe II lines of Table 2 and measured their equivalent widths with the IRAF task *splot* (see Table 3). We



**Table 2** Atomic data and equivalent widths for our selection of 15 Fe II lines

$\lambda$ nm	$\chi$ eV	$\log gf$		EW [pm]	
		H	MB	I	F
457.6340	2.84	−2.94	−2.95	6.90	6.90
462.0521	2.83	−3.21	−3.21	5.60	5.50
465.6981	2.89	−3.59	−3.60	3.60	3.50
523.4625	3.22	−2.23	−2.18	8.80	8.60
526.4812	3.23	−3.25	−3.13	4.70	4.70
541.4073	3.22	−3.50	−3.58	2.90	2.80
552.5125	3.27	−3.95	−3.97	1.35	1.25
562.7497	3.39	−4.10	−4.10	0.82	0.84
643.2680	2.89	−3.50	−3.57	4.40	4.35
651.6080	2.89	−3.38	−3.31	5.80	5.80
722.2394	3.89	−3.36	−3.26	1.95	1.92
722.4487	3.89	−3.28	−3.20	2.30	2.03
744.9335	3.89	−3.09	−3.27	1.75	1.80
751.5832	3.90	−3.44	−3.39	1.60	1.50
771.1724	3.90	−2.47	−2.50	5.30	5.12

H: Hannaford *et al.* (1992)

MB: Meléndez and Barbuy (2009)

**Table 3** Atomic data and derived abundances for our selection of 15 Fe II lines

$\lambda$ nm	$\chi$ eV	$\log gf$		A(Fe) (H MB)			
		H	MB	3D (I)	3D (F)	⟨3D⟩(I)	⟨3D⟩ (F)
457.6340	2.84	−2.94	−2.95	7.63   7.64	7.60   7.61	7.49   7.50	7.56   7.57
462.0521	2.83	−3.21	−3.21	7.54   7.54	7.48   7.48	7.43   7.43	7.45   7.45
465.6981	2.89	−3.59	−3.60	7.45   7.46	7.40   7.41	7.39   7.40	7.39   7.40
523.4625	3.22	−2.23	−2.18	7.61   7.56	7.58   7.53	7.45   7.40	7.51   7.46
526.4812	3.23	−3.25	−3.13	7.67   7.55	7.68   7.56	7.58   7.46	7.64   7.52
541.4073	3.22	−3.50	−3.58	7.45   7.53	7.42   7.50	7.40   7.48	7.40   7.48
552.5125	3.27	−3.95	−3.97	7.45   7.47	7.40   7.42	7.42   7.44	7.39   7.41
562.7497	3.39	−4.10	−4.10	7.44   7.44	7.45   7.45	7.42   7.42	7.44   7.44
643.2680	2.89	−3.50	−3.57	7.47   7.54	7.47   7.54	7.39   7.46	7.44   7.51
651.6080	2.89	−3.38	−3.31	7.67   7.60	7.69   7.62	7.56   7.49	7.64   7.57
722.2394	3.89	−3.36	−3.26	7.59   7.49	7.61   7.51	7.55   7.45	7.59   7.49
722.4487	3.89	−3.28	−3.20	7.62   7.54	7.57   7.49	7.57   7.49	7.54   7.46
744.9335	3.89	−3.09	−3.27	7.25   7.43	7.29   7.47	7.21   7.39	7.27   7.45
751.5832	3.90	−3.44	−3.39	7.56   7.51	7.54   7.49	7.52   7.47	7.52   7.47
771.1724	3.90	−2.47	−2.50	7.54   7.57	7.56   7.59	7.43   7.46	7.50   7.53
⟨A(Fe)⟩				7.53   7.53	7.52   7.51	7.46   7.45	7.49   7.48

H: Hannaford *et al.* (1992)

MB: Meléndez and Barbuy (2009)

presume that transitions from the dominant ionisation stage of iron, Fe II, are close to LTE condition (Gehren *et al.*, 2001). This is not the case for Fe I, for which NLTE effects are

important, at the level of  $\approx 0.1$  dex, as shown by Gehren *et al.* (2001), Gehren, Korn, and Shi (2001) using hydrostatic 1D model atmospheres, and by Shchukina and Bueno (2001) using a single snapshot of a 3D hydrodynamical simulation.

For the disc-centre and integrated-disc spectra, the 3D abundance that we find is  $A(\text{Fe}) = 7.525 \pm 0.057$  and  $A(\text{Fe}) = 7.512 \pm 0.062$ , respectively, when using the  $\log gf$  from Meléndez and Barbuy (2009). When we use the  $\log gf$  from Hannaford *et al.* (1992), the line-to-line scatter increases and the abundances become  $A(\text{Fe}) = 7.530 \pm 0.110$  and  $A(\text{Fe}) = 7.516 \pm 0.109$ , respectively. If we remove the 744.9 nm line, which shows an exceptionally low  $A(\text{Fe})$  value, we slightly reduce the  $\sigma$ :  $A(\text{Fe}) = 7.550 \pm 0.082$  and  $A(\text{Fe}) = 7.532 \pm 0.093$ , respectively. Thirteen of our selected Fe II lines are in common with those for which Schnabel, Kock, and Holweger (1999) have measured oscillator strengths. Using their set of  $\log gf$  values we obtain, for these 13 lines,  $A(\text{Fe})_{3D} = 7.50 \pm 0.11$  and  $A(\text{Fe})_{3D} = 7.49 \pm 0.11$  for the disc-centre and integrated-disc spectra, respectively. We conclude that the different sets of oscillator strengths provide highly consistent iron abundances. However, the line-to-line scatter is considerably smaller when adopting the Meléndez and Barbuy (2009)  $\log gf$  values. Therefore, considering both disc-centre and integrated-disc spectra, we recommend  $A(\text{Fe}) = 7.52 \pm 0.06$  for the photospheric solar iron abundance. As a consequence of the problem in representing the turbulent motions on small scales in the hydrodynamical simulations, described in Steffen, Ludwig, and Caffau (2009), there is a small slope of abundance with equivalent width of the line, which amounts to  $0.02 \text{ dex pm}^{-1}$ .

The abundances derived from the 1D models depend on the choice of the microturbulence parameter. When using the standard microturbulence value of  $\xi_{\text{mic}} = 1.0 \text{ km s}^{-1}$  and the  $\log gf$  values of Meléndez and Barbuy (2009), the abundances are  $A(\text{Fe})_{(3D)} = 7.45 \pm 0.03$ ,  $A(\text{Fe})_{\text{HM}} = 7.48 \pm 0.03$  for disc centre, and  $A(\text{Fe})_{(3D)} = 7.48 \pm 0.05$ ,  $A(\text{Fe})_{\text{HM}} = 7.50 \pm 0.05$  for the integrated disc. If we take instead the lower microturbulence values predicted by the 3D model,  $\xi_{\text{mic}} \approx 0.7 \text{ km s}^{-1}$  for disc centre, and  $\xi_{\text{mic}} \approx 0.9 \text{ km s}^{-1}$  for the integrated disc (Steffen, Ludwig, and Caffau, 2009), the resulting iron abundance is slightly higher by  $\approx 0.04$  and  $0.02$  dex, respectively.

From our analysis, the recommended solar iron abundance is  $A(\text{Fe}) = 7.52 \pm 0.06$ .

## 5.9. Europium

Basing our 3D LTE analysis (Mucciarelli *et al.*, 2008) on the five Eu II lines from Lawler *et al.* (2001), we obtain  $A(\text{Eu}) = 0.52 \pm 0.02$ . The isotopic ratio of  $^{151}\text{Eu}/(^{151}\text{Eu} + ^{153}\text{Eu})$  derived from disc-centre and integrated-disc spectra is  $(49 \pm 2.3)\%$  and  $(50 \pm 2.3)\%$ , respectively. We are in perfect agreement with the results of Lodders, Palme, and Gail (2009).

## 5.10. Hafnium

For the abundance determination of hafnium (Caffau *et al.*, 2008b), we considered four Hf II lines, suggested by Lawler *et al.* (2007). The lines are weak and blended, making the abundance determination a difficult task. Our abundance determination,  $A(\text{Hf}) = 0.87 \pm 0.04$ , is in close agreement with the photospheric value of Lodders, Palme, and Gail (2009), but larger than their meteoritic value of  $0.73 \pm 0.02$ .

## 5.11. Osmium

Osmium and iridium are among the heaviest stable elements and as such are reliable reference elements for measuring the decay of the radioactive nuclei  $^{238}\text{U}$  and  $^{232}\text{Th}$ . Therefore Os is important in radioactive cosmochronology.

The determination of the solar Os abundance is not an easy task: the suitable Os I lines lie mostly in the crowded violet and near UV range, and the transition probabilities have been revised several times in the last decades. Improved centre-of-gravity wavelengths are given by Ivarsson *et al.* (2003), who recall also that Os has seven stable isotopes; the even isotopes, which account for more than 80% of all osmium, have no hyperfine structure. However, according to the analysis of Quinet *et al.* (2006), the isotopic splitting and the hyperfine structure of the odd isotopes have no influence on the Os abundance determination.

Ivarsson *et al.* (2003) determined a new set of  $\log gf$  for 18 Os I lines and compared them with previous values, finding good agreement of their experimental results with previous determinations for the three strongest lines (290.9, 305.8, and 330.1 nm). However, a substantial disagreement is found for other lines with offset and dispersion increasing for the weaker lines. The comparison with theoretical results shows an even larger scatter. Ivarsson *et al.* (2003) did not study the solar Os abundance, but applied their new  $\log gf$  values to the analysis of the metal-poor giant CS 31082-001, previously analysed by Hill *et al.* (2002).

The solar abundance of Os has been determined by Jacoby and Aller (1976) from three Os I lines (305.8706, 330.1579, and 442.0460 nm), using  $\log gf$  from Corliss and Bozman (1962), to obtain  $A(\text{Os}) = 0.70$ . Owing to the large errors often present in the Corliss and Bozman (1962) data, a new determination of the lifetimes of nine transitions of Osmium, including the three lines used by Jacoby and Aller (1976), has been made by Kwiatkowski *et al.* (1984). These new  $\log gf$  are systematically lower than those of Corliss and Bozman (1962) (by about 0.5 dex) leading to  $A(\text{Os}) = 1.45 \pm 0.10$  from the equivalent widths of nine lines measured in the solar atlas of Delbouille, Roland, and Neven (1973), and using the HM model. This abundance agrees within one  $\sigma$  with the Os abundance in meteorites of  $A(\text{Os}) = 1.37 \pm 0.03$  (Lodders, Palme, and Gail, 2009).

The most recent transition probabilities and solar osmium abundance are due to Quinet *et al.* (2006), who also give all of the possible contaminations of each Os I line in the Sun or in metal-poor stars. New  $\log gf$  are determined by these authors for 11 Os I lines and the difference with respect to the previous results is less than 0.1 dex for all but the two lines at 397.2 nm and 442.0 nm. Their newly determined  $\log gf$  value for the 442.0 nm line differs by 0.33 from the previous value; the new  $\log gf$  value of  $-1.20$  produces an Os abundance in better agreement with that from other Os I lines in the star CS 31082-001. They determine the Os abundance using SYNTHE (Kurucz, 1993) with HM and MARCS models, but do not specify which observational data are used. They discarded not only the heavily blended lines, but also the weakest ones ( $\text{EW} < 0.2$  pm) because they are faint, sensitive to blends, and more affected by uncertainties in the  $\log gf$  values. In the end, Quinet *et al.* (2006) retained only three lines (326.7945, 330.1559, and 442.0468 nm) that give the abundances  $A(\text{Os}) = 1.40, 1.30$ , and  $1.15$ , respectively, with the HM model, and  $A(\text{Os}) = 1.30, 1.25$ , and  $1.10$  with a MARCS model. Their final Os abundance is  $A(\text{Os}) = 1.25 \pm 0.11$ .

We adopted the equivalent widths of the Os I lines from Kwiatkowski *et al.* (1984) and derived the abundances interpolating in theoretical curves-of-growth (see Table 4). We adopted the partition function from Irwin (1981) and the ionisation potential from Allen (1976). If we weight the abundances from the individual lines as in their analysis, we obtain an abundance of  $A(\text{Os})_{3\text{D}} = 1.36 \pm 0.19$ . The straight average gives  $A(\text{Os})_{3\text{D}} = 1.35 \pm 0.21$ . The  $\log gf$  values that we use are from Quinet *et al.* (2006) for all lines except for the 409 nm, 442 nm, and 463 nm lines for which we use the  $\log gf$  values from Kwiatkowski *et al.* (1984). If we restrict our selection to the three lines considered most reliable by Quinet *et al.* (2006) (330.1 nm, 409.1 nm, and 455.0 nm) we obtain a very similar value for the average ( $A(\text{Os}) = 1.37$ ) with an improved but still very large line-to-line scatter ( $\sigma = 0.16$ ). For this reason we recommend the result from the complete sample of lines.

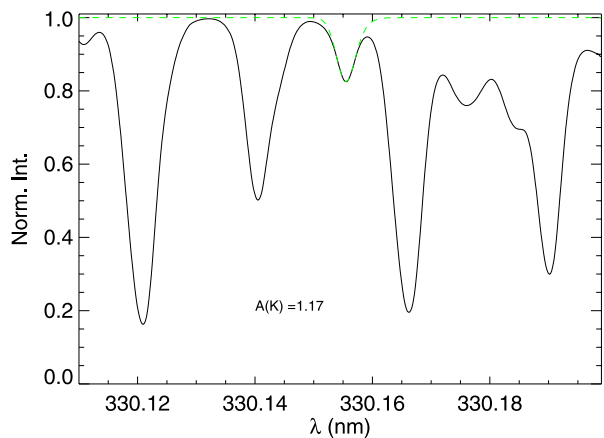
**Table 4** Os I lines used in the analysis with the abundance obtained from the EWs of disk centre using 3D, (3D), and 1D<sub>LHD</sub> model atmospheres. The microturbulence was set to 1.0 km s<sup>-1</sup> for the 1D models.

$\lambda$ nm	EW pm	$\chi$ eV	$\log gf$	$A(\text{Os})$			Weight <sup>Q</sup>
				3D	(3D)	1D <sub>LHD</sub>	
305.8660	1.03	0.00	-0.41 <sup>Q</sup>	1.070	1.069	1.020	1
326.7945	0.39	0.00	-1.09 <sup>Q</sup>	1.211	1.228	1.177	1
330.1559	0.72	0.00	-0.74 <sup>Q</sup>	1.157	1.165	1.114	3
375.2524	0.50	0.34	-0.98 <sup>Q</sup>	1.442	1.451	1.406	1
397.7231	0.07	0.64	-1.94 <sup>Q</sup>	1.777	1.789	1.744	1
409.1817	0.06	0.76	-1.66 <sup>K</sup>	1.533	1.544	1.499	3
442.0468	0.23	0.00	-1.53 <sup>K</sup>	1.195	1.218	1.165	1
455.0410	0.04	1.84	-0.71 <sup>K</sup>	1.415	1.412	1.371	3
463.1828	0.01	1.89	-1.19 <sup>K</sup>	1.332	1.329	1.288	1
$\langle A(\text{Os}) \rangle$				1.348	1.356	1.309	

Weight according to Quinet *et al.* (2006)

<sup>Q</sup> Quinet *et al.* (2006)

<sup>K</sup> Kwiatkowski *et al.* (1984)

**Figure 2** The 3D synthetic profile of the Os I line at 330.1 nm with  $A(\text{Os}) = 1.17$  (green dashed line) superimposed on the disc-centre solar atlas of Delbouille, Roland, and Neven (1973) (black solid line).

As an additional check, we fitted the profile of the line at 330.1 nm, which is the cleanest of our lines, with the (3D)+SYNTHE synthetic spectrum, allowing us to take into account all of the blending lines present in the region. The abundance we find from this fit is in very good agreement with the 1D result derived from the equivalent width. As a further illustration, we show in Figure 2 the observed profile of this line over-plotted with the 3D synthetic profile. Without the blending lines included, it is difficult to place the continuum in this case.

## 5.12. Thorium

The only line of thorium in the solar spectrum that can be used for abundance determination is the Th II resonance line at 401.9 nm (Caffau *et al.*, 2008b). This weak absorption lies on

**Table 5** The recommended abundances of the solar photosphere for the elements considered in this work.

Element	Ion. state	Abundance	N lines	Reference
Li	I	$1.03 \pm 0.03$	1	
C	I	$8.50 \pm 0.06$	45	Caffau <i>et al.</i> (2010)
N	I	$7.86 \pm 0.12$	12	Caffau <i>et al.</i> (2009)
O	I	$8.76 \pm 0.07$	10	Caffau <i>et al.</i> (2008a)
P	I	$5.46 \pm 0.04$	5	Caffau <i>et al.</i> (2007b)
S	I	$7.16 \pm 0.05$	7	Caffau and Ludwig (2007), Caffau <i>et al.</i> (2007a)
K	I	$5.11 \pm 0.09$	6	
Fe	II	$7.52 \pm 0.06$	15	
Eu	II	$0.52 \pm 0.03$	5	Mucciarelli <i>et al.</i> (2008)
Hf	II	$0.87 \pm 0.04$	4	Caffau <i>et al.</i> (2008b)
Os	I	$1.36 \pm 0.19$	9	
Th	II	$0.08 \pm 0.03$	1	Caffau <i>et al.</i> (2008b)

the red wing of a stronger Fe–Ni feature and is blended with weaker lines. We performed a line-profile-fitting analysis with a 3D synthetic profile, in order to take into account the convection-induced asymmetry of the Fe–Ni blend. Giving higher weight to the results from the disc-centre data, which resolve the line profile better, we obtained  $A(\text{Th}) = 0.08 \pm 0.03$  (Caffau *et al.*, 2008b). This result is in perfect agreement with the meteoritic value (Lodders, Palme, and Gail, 2009).

## 6. Conclusions

The abundances of the solar photosphere, based on our CO<sup>5</sup>BOLD solar model atmosphere, are reported in Table 5. We find that 3D corrections are small in general and not responsible for the systematic lowering of the solar abundances over the past years. With the abundances given in Table 5, and the abundances from Lodders, Palme, and Gail (2009), photospheric where available, for the elements that we did not analyse, we obtain a solar metallicity of  $Z = 0.0153$ , and  $Z/X = 0.0209$ . This value can be compared to  $Z = 0.0141$ , and  $Z/X = 0.0191$  of Lodders, Palme, and Gail (2009) and  $Z = 0.0134$ , and  $Z/X = 0.0181$  of Asplund *et al.* (2009).

Our spectroscopic abundances of O and Fe are in agreement, within the indicated mutual errors, with what is derived from helioseismic constraints:  $A(\text{O}) = 8.86 \pm 0.045$  and  $A(\text{Fe}) = 7.50 \pm 0.048$  (Delahaye and Pinsonneault, 2006). There is also a good agreement for the key elements C, N, and O with the most likely *spectroscopic* abundances recommended by Pinsonneault and Delahaye (2009):  $A(\text{C}) = 8.44 \pm 0.06$ ,  $A(\text{N}) = 7.96 \pm 0.10$ , and  $A(\text{O}) = 8.75 \pm 0.08$ .

We conclude that our derived solar metallicity goes in the direction of reconciling atmospheric abundances with helioseismic data. According to Turcotte and Wimmer-Schweingruber (2002), the abundance of metals in the solar photosphere may have decreased by up to 0.04 dex by diffusion during the solar lifetime. This would improve the correspondence between spectroscopic and helioseismic results even further.

**Acknowledgements** We thank Rosanna Faraggiana for her constant support and precious advice. We are grateful to Sergei Andrievsky and Sergei Korotin for NLTE computations and useful discussions. We acknowledge support from EU contract MEXT-CT-2004-014265 (CIFIST). The authors would like to thank Junwei Zhao, co-chair of the JD11 at the IAU XXVII General Assembly, for giving us the opportunity of writing this paper.

## References

- Allen, C.W.: 1976, *Astrophysical Quantities*, 3rd edn. Athlone, London.
- Asplund, M., Grevesse, N., Sauval, A.J.: 2005, In: Barnes, T.G., Bash, F.N. (eds.) *Cosmic Abundances as Records of Stellar Evolution and Nucleosynthesis* **CS-336**, Astron. Soc. Pac., San Francisco, 25.
- Asplund, M., Grevesse, N., Sauval, A.J., Allende Prieto, C., Kiselman, D.: 2004, *Astron. Astrophys.* **417**, 751.
- Asplund, M., Grevesse, N., Sauval, A.J., Scott, P.: 2009, *Annu. Rev. Astron. Astrophys.* **47**, 481.
- Ayres, T.R.: 2008, *Astrophys. J.* **686**, 731.
- Biemont, E., Baudoux, M., Kurucz, R.L., Ansbacher, W., Pinnington, E.H.: 1991, *Astron. Astrophys.* **249**, 539.
- Biémont, E., Froese Fischer, C., Godefroid, M., Vaeck, N., Hibbert, A.: 1990, In: Hansen, J.E (ed.) *3rd Int. Colloq. Roy. Netherlands Acad. Arts Sci.* 59.
- Blackwell, D.E., Lynas-Gray, A.E., Smith, G.: 1995, *Astron. Astrophys.* **296**, 217.
- Blackwell, D.E., Smith, G., Lynas-Gray, A.E.: 1995, *Astron. Astrophys.* **303**, 575.
- Bridges, J.M., Kornblith, R.L.: 1974, *Astrophys. J.* **192**, 793.
- Bridges, J.M., Wiese, W.L.: 1970, *Astrophys. J. Lett.* **161**, L71.
- Caffau, E., Ludwig, H.-G.: 2007, *Astron. Astrophys.* **467**, L11.
- Caffau, E., Ludwig, H.-G.: 2008, In: Deng, L., Chan, K.-L. (eds.) *The Art of Modeling Stars in the 21st Century, IAU Symposium 252*, Cambridge University Press, Cambridge, 35.
- Caffau, E., Ludwig, H.-G., Steffen, M.: 2009, *Mem. Soc. Astron. Ital.* **80**, 643.
- Caffau, E., Faraggiana, R., Bonifacio, P., Ludwig, H.-G., Steffen, M.: 2007a, *Astron. Astrophys.* **470**, 699.
- Caffau, E., Steffen, M., Sbordone, L., Ludwig, H.-G., Bonifacio, P.: 2007b, *Astron. Astrophys.* **473**, L9.
- Caffau, E., Ludwig, H.-G., Steffen, M., Ayres, T.R., Bonifacio, P., Cayrel, R., Freytag, B., Plez, B.: 2008a, *Astron. Astrophys.* **488**, 1031.
- Caffau, E., Sbordone, L., Ludwig, H.-G., Bonifacio, P., Steffen, M., Behara, N.T.: 2008b, *Astron. Astrophys.* **483**, 591.
- Caffau, E., Maiorca, E., Bonifacio, P., Faraggiana, R., Steffen, M., Ludwig, H.-G., Kamp, I., Busso, M.: 2009, *Astron. Astrophys.* **498**, 877.
- Caffau, E., Ludwig, H., Bonifacio, P., Faraggiana, R., Steffen, M., Freytag, B., Kamp, I., Ayres, T.R.: 2010, *Astron. Astrophys.* doi:[10.1051/0004-6361/200912227](https://doi.org/10.1051/0004-6361/200912227)
- Corliss, C.H., Bozman, W.R.: 1962, *Experimental Transition Probabilities for Spectral Lines of Seventy Elements; Derived from the NBS Tables of Spectral-Line Intensities*, US Department of Commerce, National Bureau of Standards, Washington.
- Corliss, C.H., Tech, J.L.: 1968, *NBS Monograph 108*, US Dept. of Commerce, National Bureau of Standards, Washington.
- Corliss, C.H., Warner, B.: 1966, *J. Res. NBS – A* **70**, 325.
- de La Reza, R., Müller, E.A.: 1975, *Solar Phys.* **43**, 15.
- Delahaye, F., Pinsonneault, M.H.: 2006, *Astrophys. J.* **649**, 529.
- Delbouille, L., Roland, G., Neven, L.: 1973, *Atlas Photométrique du Spectre Solaire de  $\lambda$ 3000 à  $\lambda$ 10 000*, Université de Liège, Institut d'Astrophysique, Liège.
- Delbouille, L., Roland, G., Brault, J.W., Testerman, L.: 1981, Photometric atlas of the solar spectrum from 1850 to 10 000  $\text{cm}^{-1}$ . [http://bass2000.obspm.fr/solar\\_spect.php](http://bass2000.obspm.fr/solar_spect.php).
- Freytag, B., Steffen, M., Dorch, B.: 2002, *Astron. Nachr.* **323**, 213.
- Freytag, B., Steffen, M., Wedemeyer-Böhm, S., Ludwig, H.-G.: 2003, CO5BOLD User Manual. [http://www.astro.uu.se/~bf/co5bold\\_main.html](http://www.astro.uu.se/~bf/co5bold_main.html).
- Gehren, T., Korn, A.J., Shi, J.: 2001, *Astron. Astrophys.* **380**, 645.
- Gehren, T., Butler, K., Mashonkina, L., Reetz, J., Shi, J.: 2001, *Astron. Astrophys.* **366**, 981.
- Ghezzi, L., Cunha, K., Smith, V.V., Margheim, S., Schuler, S., de Araújo, F.X., de la Reza, R.: 2009, *Astrophys. J.* **698**, 451.
- Grevesse, N., Sauval, A.J.: 1999, *Astron. Astrophys.* **347**, 348.
- Grevesse, N., Lambert, D.L., Sauval, A.J., van Dishoeck, E.F., Farmer, C.B., Norton, R.H.: 1990, *Astron. Astrophys.* **232**, 225.
- Hannaford, P., Lowe, R.M., Grevesse, N., Noels, A.: 1992, *Astron. Astrophys.* **259**, 301.

- Hill, V., Plez, B., Cayrel, R., Beers, T.C., Nordström, B., Andersen, J., Spite, M., Spite, F., Barbuy, B., Bonifacio, P., Depagne, E., François, P., Primas, F.: 2002, *Astron. Astrophys.* **387**, 560.
- Holweger, H.: 1967, *Z. Astrophys.* **65**, 365.
- Holweger, H., Kock, M., Bard, A.: 1995, *Astron. Astrophys.* **296**, 233.
- Holweger, H., Müller, E.A.: 1974, *Solar Phys.* **39**, 19.
- Irwin, A.W.: 1981, *Astrophys. J. Suppl. Ser.* **45**, 621.
- Ivanova, D.V., Shimanskii, V.V.: 2000, *Astron. Rep.* **44**, 376.
- Ivarsson, S., Andersen, J., Nordström, B., Dai, X., Johansson, S., Lundberg, H., Nilsson, H., Hill, V., Lundqvist, M., Wyart, J.F.: 2003, *Astron. Astrophys.* **409**, 1141.
- Jacoby, G., Aller, L.H.: 1976, *Proc. Natl. Acad. Sci.* **73**, 1382.
- Korotin, S.A.: 2008, *Odessa Astron. Publ.* **21**, 42.
- Korotin, S.A.: 2009, *Astron. Rep.* **53**, 651.
- Kostik, R.I., Shchukina, N.G., Rutten, R.J.: 1996, *Astron. Astrophys.* **305**, 325.
- Kurucz, R.: 1993, *SYNTHES Spectrum Synthesis Programs and Line Data. Kurucz CD-ROM 18*, Smithsonian Astrophysical Observatory, Cambridge.
- Kurucz, R.L.: 2005, *Mem. Soc. Astron. Ital. Suppl.* **8**, 189.
- Kwiatkowski, M., Zimmermann, P., Biemont, E., Grevesse, N.: 1984, *Astron. Astrophys.* **135**, 59.
- Lambert, D.L.: 1978, *Mon. Not. Roy. Astron. Soc.* **182**, 249.
- Lambert, D.L., Luck, R.E.: 1978, *Mon. Not. Roy. Astron. Soc.* **183**, 79.
- Lawler, J.E., Wickliffe, M.E., den Hartog, E.A., Sneden, C.: 2001, *Astrophys. J.* **563**, 1075.
- Lawler, J.E., den Hartog, E.A., Labby, Z.E., Sneden, C., Cowan, J.J., Ivans, I.I.: 2007, *Astrophys. J. Suppl. Ser.* **169**, 120.
- Lodders, K., Palme, H., Gail, H.-P.: 2009, *Astronomy, Astrophysics, and Cosmology, B: Solar System, Landolt – Börnstein, New Series VI/4*, Springer, Berlin, 560.
- Ludwig, H.-G., Caffau, E., Steffen, M., Bonifacio, P., Freytag, B., Cayrel, R.: 2010, *IAU Symp.* **265**, 201. doi:[10.1017/S1743921310000542](https://doi.org/10.1017/S1743921310000542).
- Maiorca, E., Caffau, E., Bonifacio, P., Busso, M., Faraggiana, R., Steffen, M., Ludwig, H.-G., Kamp, I.: 2009, *Publ. Astron. Soc. Aust.* **26**, 345.
- Meléndez, J., Barbuy, B.: 2009, *Astron. Astrophys.* **497**, 611.
- Mucciarelli, A., Caffau, E., Freytag, B., Ludwig, H.-G., Bonifacio, P.: 2008, *Astron. Astrophys.* **484**, 841.
- Neckel, H.: 1999, *Solar Phys.* **184**, 421.
- Neckel, H., Labs, D.: 1984, *Solar Phys.* **90**, 205.
- Pinsonneault, M.H., Delahaye, F.: 2009, *Astrophys. J.* **704**, 1174.
- Quinet, P., Palmeri, P., Biémont, É., Jorissen, A., van Eck, S., Svanberg, S., Xu, H.L., Plez, B.: 2006, *Astron. Astrophys.* **448**, 1207.
- Reddy, B.E., Lambert, D.L., Laws, C., Gonzalez, G., Covey, K.: 2002, *Mon. Not. Roy. Astron. Soc.* **335**, 1005.
- Russell, H.N.: 1929, *Astrophys. J.* **70**, 11.
- Ryde, N.: 2006, *Astron. Astrophys.* **455**, L13.
- Schnabel, R., Kock, M., Holweger, H.: 1999, *Astron. Astrophys.* **342**, 610.
- Shchukina, N., Trujillo Bueno, J.: 2001, *Astrophys. J.* **550**, 970.
- Steenbock, W., Holweger, H.: 1984, *Astron. Astrophys.* **130**, 319.
- Steffen, M., Holweger, H.: 2002, *Astron. Astrophys.* **387**, 258.
- Steffen, M., Ludwig, H.-G., Caffau, E.: 2009, *Mem. Soc. Astron. Ital.* **80**, 731.
- Takeda, Y., Kato, K.-I., Watanabe, Y., Sadakane, K.: 1996, *Publ. Astron. Soc. Japan* **48**, 511.
- Takeda, Y., Hashimoto, O., Taguchi, H., Yoshioka, K., Takada-Hidai, M., Saito, Y., Honda, S.: 2005, *Publ. Astron. Soc. Japan* **57**, 751.
- Turcotte, S., Wimmer-Schweingruber, R.F.: 2002, *J. Geophys. Res. A* **107**, 1442.
- Zhang, H.W., Butler, K., Gehren, T., Shi, J.R., Zhao, G.: 2006, *Astron. Astrophys.* **453**, 723.